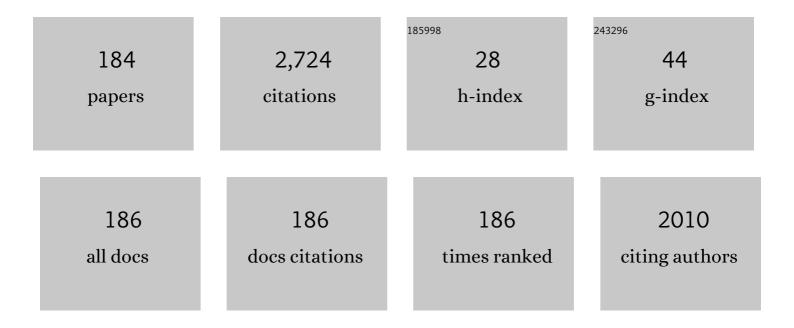
List of Publications by Year in descending order

Source: https://exaly.com/author-pdf/4974884/publications.pdf Version: 2024-02-01



#	Article	IF	CITATIONS
1	Anomalous reduction of thermal conductivity in coherent nanocrystal architecture for silicon thermoelectric material. Nano Energy, 2015, 12, 845-851.	8.2	150
2	An Approach to Ideal Semiconductor Electrodes for Efficient Photoelectrochemical Reduction of Carbon Dioxide by Modification with Small Metal Particles. Journal of Physical Chemistry B, 1998, 102, 974-980.	1.2	144
3	Observation of the quantum-confinement effect in individual Ge nanocrystals on oxidized Si substrates using scanning tunneling spectroscopy. Applied Physics Letters, 2005, 87, 133119.	1.5	112
4	Quantum-confinement effect in individual Ge1â~xSnx quantum dots on Si(111) substrates covered with ultrathin SiO2 films using scanning tunneling spectroscopy. Applied Physics Letters, 2007, 91, .	1.5	82
5	Self-Consistent Density Functional Calculation of Field Emission Currents from Metals. Physical Review Letters, 2000, 85, 1750-1753.	2.9	74
6	Methodology of Thermoelectric Power Factor Enhancement by Controlling Nanowire Interface. ACS Applied Materials & Interfaces, 2018, 10, 37709-37716.	4.0	72
7	Phonon transport control by nanoarchitecture including epitaxial Ge nanodots for Si-based thermoelectric materials. Scientific Reports, 2015, 5, 14490.	1.6	71
8	Nanostructure design for drastic reduction of thermal conductivity while preserving high electrical conductivity. Science and Technology of Advanced Materials, 2018, 19, 31-43.	2.8	69
9	A reproducible method to fabricate atomically sharp tips for scanning tunneling microscopy. Review of Scientific Instruments, 1999, 70, 3373-3376.	0.6	59
10	Self-organized formation and self-repair of a two-dimensional nanoarray of Ge quantum dots epitaxially grown on ultrathin SiO ₂ -covered Si substrates. Nanotechnology, 2010, 21, 095305.	1.3	58
11	Epitaxial Growth of High Quality Ge Films on Si(001) Substrates by Nanocontact Epitaxy. Crystal Growth and Design, 2011, 11, 3301-3305.	1.4	48
12	Nanoscale Imaging of Electronic Surface Transport Probed by Atom Movements Induced by Scanning Tunneling Microscope Current. Physical Review Letters, 2002, 89, 266805.	2.9	46
13	Independent control of electrical and heat conduction by nanostructure designing for Si-based thermoelectric materials. Scientific Reports, 2016, 6, 22838.	1.6	45
14	Ultimate Confinement of Phonon Propagation in Silicon Nanocrystalline Structure. Physical Review Letters, 2018, 120, 045901.	2.9	45
15	Quantum fluctuation of tunneling current in individual Ge quantum dots induced by a single-electron transfer. Applied Physics Letters, 2007, 90, 153104.	1.5	44
16	Epitaxial growth of ultrahigh density Ge1â^'xSnx quantum dots on Si (111) substrates by codeposition of Ge and Sn on ultrathin SiO2 films. Journal of Applied Physics, 2007, 102, 124302.	1.1	43
17	Formation of ultrahigh density and ultrasmall coherent βâ€FeSi2 nanodots on Si (111) substrates using Si and Fe codeposition method. Journal of Applied Physics, 2006, 100, 044313.	1.1	40
18	Thermoelectric power factor enhancement based on carrier transport physics in ultimately phonon-controlled Si nanostructures. Materials Today Energy, 2019, 13, 56-63.	2.5	39

#	Article	IF	CITATIONS
19	Formation of strained iron silicide nanodots by Fe deposition on Si nanodots on oxidized Si (111) surfaces. Physical Review B, 2005, 72, .	1.1	36
20	High Thermoelectric Power Factor Realization in Si-Rich SiGe/Si Superlattices by Super-Controlled Interfaces. ACS Applied Materials & Interfaces, 2020, 12, 25428-25434.	4.0	36
21	Quantum confinement observed in Ge nanodots on an oxidized Si surface. Physical Review B, 2006, 73, .	1.1	35
22	Nanocontact heteroepitaxy of thin GaSb and AlGaSb films on Si substrates using ultrahigh-density nanodot seeds. Nanotechnology, 2011, 22, 265301.	1.3	33
23	In situ scanning tunneling microscopic study of polymerization of C60 clusters induced by electron injection from the probe tips. Applied Physics Letters, 2000, 77, 2834-2836.	1.5	30
24	Low thermal conductivity in single crystalline epitaxial germanane films. Applied Physics Express, 2020, 13, 055503.	1.1	30
25	Carrier and phonon transport control by domain engineering for high-performance transparent thin film thermoelectric generator. Applied Physics Letters, 2021, 118, .	1.5	30
26	Cluster reactions in C60 films induced by electron injection from a scanning tunneling microscope tip. Surface Science, 2003, 528, 151-155.	0.8	29
27	Photoluminescence of Geâ^•Si structures grown on oxidized Si surfaces. Applied Physics Letters, 2006, 88, 121919.	1.5	29
28	Self-Assembled Epitaxial Growth of High Density β-FeSi ₂ Nanodots on Si (001) and Their Spatially Resolved Optical Absorption Properties. Crystal Growth and Design, 2008, 8, 3019-3023.	1.4	29
29	Formation of ultrahigh density Ge nanodots on oxidized Ge/Si(111) surfaces. Journal of Applied Physics, 2004, 95, 5014-5018.	1.1	28
30	Enhanced thermoelectric performance of Ga-doped ZnO film by controlling crystal quality for transparent thermoelectric films. Thin Solid Films, 2018, 666, 185-190.	0.8	28
31	Formation and optical properties of GaSb quantum dots epitaxially grown on Si substrates using an ultrathin SiO2 film technique. Journal of Applied Physics, 2009, 105, .	1.1	27
32	Resistive switching memory performance in oxide hetero-nanocrystals with well-controlled interfaces. Science and Technology of Advanced Materials, 2020, 21, 195-204.	2.8	27
33	Nonthermal decomposition of C60 polymers induced by tunneling electron injection. Applied Physics Letters, 2004, 85, 5242-5244.	1.5	26
34	Influence of growth and annealing conditions on photoluminescence of Ge/Si layers grown on oxidized Si surfaces. Journal of Physics Condensed Matter, 2007, 19, 136004.	0.7	26
35	Photoluminescence of Si layers grown on oxidized Si surfaces. Journal of Applied Physics, 2007, 101, 033532.	1.1	26
36	Giant Enhancement of Seebeck Coefficient by Deformation of Silicene Buckled Structure in Calciumâ€Intercalated Layered Silicene Film. Advanced Materials Interfaces, 2022, 9, 2101752.	1.9	26

#	Article	IF	CITATIONS
37	Observation of the quantum-confinement effect in individual β-FeSi2 nanoislands epitaxially grown on Si (111) surfaces using scanning tunneling spectroscopy. Applied Physics Letters, 2006, 89, 123104.	1.5	24
38	Diffusion of chlorine atoms on Si(111)-(7×7) surface enhanced by electron injection from scanning tunneling microscope tips. Surface Science, 2001, 487, 127-134.	0.8	23
39	Phonon transport in the nano-system of Si and SiGe films with Ge nanodots and approach to ultralow thermal conductivity. Nanoscale, 2021, 13, 4971-4977.	2.8	22
40	Photoluminescence from Si-capped GeSn nanodots on Si substrates formed using an ultrathin SiO2 film technique. Journal of Applied Physics, 2009, 106, 014309.	1.1	21
41	Defect-related light emission in the 1.4–1.7â€,μm range from Si layers at room temperature. Journal of Applied Physics, 2009, 105, .	1.1	20
42	Embedded-ZnO Nanowire Structure for High-Performance Transparent Thermoelectric Materials. Journal of Electronic Materials, 2017, 46, 3020-3024.	1.0	20
43	Anomalous enhancement of thermoelectric power factor by thermal management with resonant level effect. Journal of Materials Chemistry A, 2021, 9, 4851-4857.	5.2	20
44	Thermoelectric Si1â^' <i>x</i> Ge <i>x</i> and Ge epitaxial films on Si(001) with controlled composition and strain for group IV element-based thermoelectric generators. Applied Physics Letters, 2020, 117, .	1.5	19
45	STM Images Apparently Corresponding to a Stable Structure: Considerable Fluctuation of a Phase Boundary of the Si(111)-(3×3)-Ag Surface. Physical Review Letters, 2001, 87, 156102.	2.9	18
46	Hopping motion of chlorine atoms on Si(100)-(2×1) surfaces induced by carrier injection from scanning tunneling microscope tips. Surface Science, 2003, 531, 68-76.	0.8	17
47	Strength distribution of titania ceramics after high-voltage screening. Journal of Materials Science, 1996, 31, 3419-3425.	1.7	16
48	Spreading effects in surface reactions induced by tunneling current injection from an STM tip. Surface Science, 2003, 528, 110-114.	0.8	16
49	Fourier-transform photoabsorption spectroscopy of quantum-confinement effects in individual GeSn nanodots. Applied Physics Letters, 2009, 94, 093104.	1.5	16
50	Molecular dynamics study of deposition mechanism of cubic boron nitride. Science and Technology of Advanced Materials, 2001, 2, 349-356.	2.8	15
51	Dislocation confinement in the growth of Na flux GaN on metalorganic chemical vapor deposition-GaN. Journal of Applied Physics, 2015, 118, .	1.1	15
52	Thermoelectric Properties of Epitaxial β-FeSi2 Thin Films on Si(111) and Approach for Their Enhancement. Journal of Electronic Materials, 2017, 46, 3235-3241.	1.0	15
53	Significant reduction in the thermal conductivity of Si-substituted <mml:math xmlns:mml="http://www.w3.org/1998/Math/MathML"> <mml:mrow> <mml:msub> <mml:mi> Fe</mml:mi> <mml: epilayers. Physical Review B, 2019, 99, .</mml: </mml:msub></mml:mrow></mml:math 	mn x2k/mr	nl:ma>
54	Methodology of Thermoelectric Power Factor Enhancement by Nanoscale Thermal Management in Bulk SiGe Composites. ACS Applied Energy Materials, 2020, 3, 1235-1241.	2.5	14

#	Article	IF	CITATIONS
55	Chlorine atom diffusion on Si()-(7×7) surface enhanced by hole injection from scanning tunneling microscope tips. Surface Science, 2002, 497, 166-170.	0.8	13
56	Structural change of radiation defects in graphite crystals induced by STM probing. Applied Physics A: Materials Science and Processing, 2002, 74, 311-316.	1.1	13
57	Desorption of chlorine atoms on Si (111)-(7×7) surfaces induced by hole injection from scanning tunneling microscope tips. Surface Science, 2007, 601, 2189-2193.	0.8	13
58	Fabrication of Si Thermoelectric Nanomaterials Containing Ultrasmall Epitaxial Ge Nanodots with an Ultrahigh Density. Journal of Electronic Materials, 2015, 44, 2015-2020.	1.0	13
59	Fabrication of Carrier-Doped Si Nanoarchitecture for Thermoelectric Material by Ultrathin SiO2 Film Technique. Journal of Electronic Materials, 2016, 45, 1914-1920.	1.0	13
60	Arbitrary cross-section SEM-cathodoluminescence imaging of growth sectors and local carrier concentrations within micro-sampled semiconductor nanorods. Nature Communications, 2016, 7, 10609.	5.8	13
61	High thermoelectric performance in high crystallinity epitaxial Si films containing silicide nanodots with low thermal conductivity. Applied Physics Letters, 2019, 115, 182104.	1.5	13
62	Atomic and electronic structure of the Si(111)-â^š3xâ^š3-Ag surface reexamined using first-principles calculations. Science and Technology of Advanced Materials, 2000, 1, 167-172.	2.8	12
63	Ultrathin-body Ge-on-insulator wafers fabricated with strongly bonded thin Al ₂ O ₃ /SiO ₂ hybrid buried oxide layers. Applied Physics Express, 2014, 7, 086501.	1.1	12
64	Low thermal conductivity of thermoelectric Fe ₂ VAl films. Applied Physics Express, 2017, 10, 115802.	1.1	12
65	Thermoelectric properties of single-phase full-Heusler alloy Fe2TiSi films with <i>D</i> 3-type disordering. Journal of Applied Physics, 2020, 127, .	1.1	12
66	Measurements of local optical properties of Si-doped GaAs (110) surfaces using modulation scanning tunneling microscope cathodoluminescence spectroscopy. Journal of Vacuum Science & Technology B, 2008, 26, 195.	1.3	11
67	Fabrication of bonded GeOI substrates with thin Al2O3/SiO2 buried oxide layers. Solid-State Electronics, 2013, 83, 42-45.	0.8	11
68	Epitaxial multilayers of β-FeSi2 nanodots/Si for Si-based nanostructured electronic materials. Journal of Vacuum Science and Technology A: Vacuum, Surfaces and Films, 2017, 35, 041402.	0.9	11
69	Thermal Conductivity Measurement of Thermoelectric Thin Films by a Versatility-Enhanced 2ï‰ Method. Journal of Electronic Materials, 2017, 46, 3089-3096.	1.0	11
70	Resistive switching at the high quality metal/insulator interface in Fe3O4/SiO2/ <i>α</i> -FeSi2/Si stacking structure. Applied Physics Letters, 2018, 113, .	1.5	11
71	Bottomâ€Up Onâ€5urface Synthesis of Twoâ€Dimensional Graphene Nanoribbon Networks and Their Thermoelectric Properties. Chemistry - an Asian Journal, 2019, 14, 4400-4407.	1.7	11
72	Nanostructure design for high performance thermoelectric materials based on anomalous Nernst effect using metal/semiconductor multilayer. Applied Physics Express, 2021, 14, 075002.	1.1	11

#	Article	IF	CITATIONS
73	Polymerization and depolymerization of fullerenes induced by hole injection from scanning tunneling microscope tips. Surface Science, 2007, 601, 5207-5211.	0.8	10
74	Luminescence at 1.5µm from Si/GeSn nanodot/Si structures. Journal Physics D: Applied Physics, 2012, 45, 035304.	1.3	10
75	Cross-sectional X-ray microdiffraction study of a thick AlN film grown on a trench-patterned AlN/α-Al2O3 template. Journal of Crystal Growth, 2013, 381, 37-42.	0.7	10
76	Epitaxial iron oxide nanocrystals with memory function grown on Si substrates. Applied Physics Express, 2016, 9, 055508.	1.1	10
77	An advanced 2ω method enabling thermal conductivity measurement for various sample thicknesses: From thin films to bulk materials. Journal of Applied Physics, 2020, 128, 015102.	1.1	10
78	Fourier transform photoabsorption spectroscopy based on scanning tunneling microscopy. Journal of Applied Physics, 2007, 102, .	1.1	9
79	Control of epitaxial growth of Fe-based nanocrystals on Si substrates using well-controlled nanometer-sized interface. Journal of Applied Physics, 2014, 115, 044301.	1.1	9
80	Effect of Fe–V nonstoichiometry on electrical and thermoelectric properties of Fe ₂ VAl films. Japanese Journal of Applied Physics, 2018, 57, 040306.	0.8	9
81	Impact of metal silicide nanocrystals on the resistance ratio in resistive switching of epitaxial Fe3O4 films on Si substrates. Applied Physics Letters, 2020, 116, .	1.5	9
82	Thermoelectric power factor enhancement of calcium-intercalated layered silicene by introducing metastable phase. Applied Physics Express, 2021, 14, 115505.	1.1	9
83	Quantum-Size Effect in Uniform Ge–Sn Alloy Nanodots Observed by Photoemission Spectroscopy. Japanese Journal of Applied Physics, 2007, 46, L1176.	0.8	8
84	The origin of spectral distortion in electric field modulation spectroscopy based on scanning tunneling microscopy. Surface Science, 2007, 601, 5300-5303.	0.8	8
85	Spatial resolution of imaging contaminations on the GaAs surface by scanning tunneling microscope-cathodoluminescence spectroscopy. Applied Surface Science, 2008, 254, 7737-7741.	3.1	8
86	Fe3Si nanodots epitaxially grown on Si(111) substrates using ultrathin SiO2 film technique. Thin Solid Films, 2011, 519, 8512-8515.	0.8	8
87	Electrical Characterization of Wafer-Bonded Germanium-on-Insulator Substrates Using a Four-Point-Probe Pseudo-Metal–Oxide–Semiconductor Field-Effect Transistor. Japanese Journal of Applied Physics, 2011, 50, 04DA14.	0.8	8
88	Vertical dislocations in Ge films selectively grown in submicron Si windows of patterned substrates. Thin Solid Films, 2012, 520, 3245-3248.	0.8	8
89	Influence of nanometer-sized interface on reaction of iron nanocrystals epitaxially grown on silicon substrates with oxygen gas. Journal of Applied Physics, 2013, 114, .	1.1	8
90	Microscopic crystalline structure of a thick AlN film grown on a trench-patterned AlN/α-Al2O3 template. Journal of Crystal Growth, 2015, 411, 38-44.	0.7	8

#	Article	IF	CITATIONS
91	Thermoelectric properties of epitaxial Ge thin films on Si(001) with strong crystallinity dependence. Applied Physics Express, 2018, 11, 111301.	1.1	8
92	Heat transport through propagon-phonon interaction in epitaxial amorphous-crystalline multilayers. Communications Physics, 2021, 4, .	2.0	8
93	Title is missing!. Journal of Materials Science, 1999, 34, 4233-4237.	1.7	7
94	Evidence of negative leaders prior to fast rise ICC pulses of upward lightning. Journal of Atmospheric Electricity, 2009, 29, 13-21.	0.1	7
95	Scanning tunneling microscope–cathodoluminescence measurement of the GaAs/AlGaAs heterostructure. Journal of Vacuum Science & Technology B, 2009, 27, 1874.	1.3	7
96	Structural change of direct silicon bonding substrates by interfacial oxide out-diffusion annealing. Thin Solid Films, 2010, 518, S147-S150.	0.8	7
97	Luminescence properties of Si-capped <i>î²</i> -FeSi2 nanodots epitaxially grown on Si(001) and (111) substrates. Journal of Applied Physics, 2014, 115, .	1.1	7
98	Resistive switching characteristics of isolated core-shell iron oxide/germanium nanocrystals epitaxially grown on Si substrates. Applied Physics Letters, 2018, 112, .	1.5	7
99	Structural Analysis of Si-Based Nanodot Arrays Self-Organized by Selective Etching of SiGe/Si Films. Japanese Journal of Applied Physics, 2011, 50, 08LB11.	0.8	7
100	Low thermal conductivity of complex thermoelectric barium silicide film epitaxially grown on Si. Applied Physics Letters, 2021, 119, .	1.5	7
101	Manipulating Ge quantum dots on ultrathin SixGe1â^'x oxide films using scanning tunneling microscope tips. Surface Science, 2006, 600, 3456-3460.	0.8	6
102	Electric field modulation nanospectroscopy for characterization of individual β-FeSi2 nanodots. Journal of Applied Physics, 2008, 104, .	1.1	6
103	Formation and Magnetic Properties of Ultrahigh Density Fe3Si Nanodots Epitaxially Grown on Si(111) Substrates Covered with Ultrathin SiO2Films. Japanese Journal of Applied Physics, 2011, 50, 015501.	0.8	6
104	Annealing Effects on Ge/SiO2Interface Structure in Wafer-Bonded Germanium-on-Insulator Substrates. Japanese Journal of Applied Physics, 2011, 50, 04DA13.	0.8	6
105	Electrical characterization of wafer-bonded Ge(111)-on-insulator substrates using four-point-probe pseudo-metal-oxide-semiconductor field-effect transistor method. Thin Solid Films, 2012, 520, 3232-3235.	0.8	6
106	Crystalline property analysis of semipolar (20–21) GaN on (22–43) patterned sapphire substrate by Xâ€ray microdiffraction and transmission electron microscopy. Physica Status Solidi (B): Basic Research, 2015, 252, 1149-1154.	0.7	6
107	Phase diagram of the Bi2O3-SrO-CaO quasiternary system. Metallurgical and Materials Transactions A: Physical Metallurgy and Materials Science, 1993, 24, 1447-1449.	1.1	5
108	Characterization of semiconductor nanostructures formed by using ultrathin Si oxide technology. Applied Surface Science, 2008, 255, 669-671.	3.1	5

#	Article	IF	CITATIONS
109	Impact ionization of excitons in Ge/Si structures with Ge quantum dots grown on the oxidized Si(100) surfaces. Journal of Applied Physics, 2014, 115, 203702.	1.1	5
110	Thickness and growth condition dependence of crystallinity in semipolar (20–21) GaN films grown on (22–43) patterned sapphire substrates. Physica Status Solidi (B): Basic Research, 2015, 252, 1142-1148.	0.7	5
111	Effect of Fe coating of nucleation sites on epitaxial growth of Fe oxide nanocrystals on Si substrates. Japanese Journal of Applied Physics, 2016, 55, 08NB12.	0.8	5
112	Thermoelectric properties of epitaxial β-FeSi ₂ thin films grown on Si(111) substrates with various film qualities. Japanese Journal of Applied Physics, 2017, 56, 05DC04.	0.8	5
113	Growth of epitaxial FeGeÎ ³ nanocrystals with incommensurate Nowotny chimney-ladder phase on Si substrate. Japanese Journal of Applied Physics, 2018, 57, 08NB01.	0.8	5
114	Control of thermoelectric properties in Mn-substituted <mml:math xmlns:mml="http://www.w3.org/1998/Math/MathML"> <mml:mrow> <mml:msub> <mml:mi> Fe</mml:mi> <mml:r epilayers. Physical Review B, 2020, 102, .</mml:r </mml:msub></mml:mrow></mml:math 	mn a2 k/mr	nl:nøn>
115	Annealing Effects on Ge/SiO2Interface Structure in Wafer-Bonded Germanium-on-Insulator Substrates. Japanese Journal of Applied Physics, 2011, 50, 04DA13.	0.8	5
116	Electrical Characterization of Wafer-Bonded Germanium-on-Insulator Substrates Using a Four-Point-Probe Pseudo-Metal–Oxide–Semiconductor Field-Effect Transistor. Japanese Journal of Applied Physics, 2011, 50, 04DA14.	0.8	5
117	Starin dependent electrical resistance of carbon-insulator composite. Journal of Materials Science Letters, 1994, 13, 829-831.	0.5	4
118	Spatially Extended Polymerization of C 60 Clusters Induced by Localized Current Injection from Scanning Tunneling Microscope Tips. Molecular Crystals and Liquid Crystals, 2002, 386, 135-138.	0.4	4
119	Role of Intermolecular Separation in Nanoscale Patterning C60Films by Local Injection of Electrons from Scanning Tunneling Microscope Tip. Japanese Journal of Applied Physics, 2005, 44, L1373-L1376.	0.8	4
120	Giant fullerenes formed on C60 films irradiated with electrons field-emitted from scanning tunneling microscope tips. Applied Surface Science, 2008, 254, 7881-7884.	3.1	4
121	High resolution transmission electron microscopy study of iron-silicide nanodot structures grown on faintly oxidized Si (111) surfaces. Thin Solid Films, 2009, 517, 2865-2870.	0.8	4
122	X-ray microdiffraction investigation of crystallinity and strain relaxation in Ge thin lines selectively grown on Si(001) substrates. Solid-State Electronics, 2011, 60, 26-30.	0.8	4
123	Characterization of Ge Films on Si(001) Substrates Grown by Nanocontact Epitaxy. Japanese Journal of Applied Physics, 2013, 52, 095503.	0.8	4
124	Self-assembly of Ge clusters on highly oriented pyrolytic graphite surfaces. Surface Science, 2014, 628, 82-85.	0.8	4
125	Nanostructural effect on thermoelectric properties in Si films containing iron silicide nanodots. Japanese Journal of Applied Physics, 2020, 59, SFFB01.	0.8	4
126	Anomalous Enhancement of IR Emission in Zn1?xMnxS Retrieved after Pressure-Induced Phase Transition. Physica Status Solidi (B): Basic Research, 1999, 211, 359-364.	0.7	3

#	Article	IF	CITATIONS
127	The enhanced signal of subgap centers in tip-probing photoabsorption spectroscopy with an assist of a subsidiary light. Journal of Applied Physics, 2008, 103, 044303.	1.1	3
128	Conductive optical-fiber STM probe for local excitation and collection of cathodoluminescence at semiconductor surfaces. Optics Express, 2013, 21, 19261.	1.7	3
129	Investigating the origin of intense photoluminescence in Si capping layer on Ge1â^'xSnx nanodots by transmission electron microscopy. Journal of Applied Physics, 2013, 113, 074302.	1.1	3
130	Anisotropic crystalline morphology of epitaxial thick AlN films grown on triangular-striped AlN/sapphire template. Physica Status Solidi (A) Applications and Materials Science, 2014, 211, 731-735.	0.8	3
131	Formation and optical properties of Ge films grown on Si(111) substrates using nanocontact epitaxy. Applied Surface Science, 2015, 325, 170-174.	3.1	3
132	Amorphous/epitaxial superlattice for thermoelectric application. Japanese Journal of Applied Physics, 2016, 55, 081201.	0.8	3
133	Protosymbol emergence based on embodiment: robot experiments. , 0, , .		2
134	Structural Analysis of Si-Based Nanodot Arrays Self-Organized by Selective Etching of SiGe/Si Films. Japanese Journal of Applied Physics, 2011, 50, 08LB11.	0.8	2
135	Self-organization of two-dimensional SiGe nanodot arrays using selective etching of pure-edge dislocation network. Journal of Applied Physics, 2011, 109, 044301-044301-4.	1.1	2
136	Areal density control of ZnO nanowires in physical vapor transport using Ge nanocrystals. Japanese Journal of Applied Physics, 2018, 57, 08NB07.	0.8	2
137	Modulation of lattice constants by changing the composition and strain in incommensurate Nowotny chimney-ladder phase FeGe epitaxially grown on Si. Surface Science, 2019, 690, 121470.	0.8	2
138	Semiconductor Nanostructure Design for Thermoelectric Property Control. International Journal of Nanoscience, 2019, 18, 1940036.	0.4	2
139	Formation of Silicon Quantum Dots Sheet on a Nonmetallic CaF 2 Surface. Advanced Materials Interfaces, 2020, 7, 2001295.	1.9	2
140	Direct mapping of temperature-difference-induced potential variation under non-thermal equilibrium. Applied Physics Letters, 2021, 118, 091605.	1.5	2
141	Synergistic phonon scattering in epitaxial silicon multilayers with germanium nanodot inclusions. Physical Review B, 2021, 104, .	1.1	2
142	The Effect of Ethanol on Disassembly of Amyloid-β1-42 Pentamer Revealed by Atomic Force Microscopy and Gel Electrophoresis. International Journal of Molecular Sciences, 2022, 23, 889.	1.8	2
143	Seed-assisted epitaxy of intermetallic compounds with interface-determined orientation: Incommensurate Nowotny chimney-ladder FeGe epitaxial film. Acta Materialia, 2022, 236, 118130.	3.8	2
144	Title is missing!. Journal of Materials Science Letters, 1999, 18, 1159-1161.	0.5	1

#	Article	IF	CITATIONS
145	STM observations of photo-induced jumps of chlorine atoms chemisorbed on Si(111)-(7×7) surface. Surface Science, 2005, 593, 155-160.	0.8	1
146	X-ray Microdiffraction Study on Crystallinity of Micron-Sized Ge Films Selectively Grown on Si(001) Substrates. ECS Transactions, 2010, 33, 887-892.	0.3	1
147	Microscopic Structure of Directly Bonded Silicon Substrates. Key Engineering Materials, 0, 470, 164-170.	0.4	1
148	Scanning tunneling microscope-based local electroluminescence spectroscopy of p-AlGaAs/i-GaAs/n-AlGaAs double heterostructure. Journal of Vacuum Science and Technology B:Nanotechnology and Microelectronics, 2012, 30, 021802.	0.6	1
149	(Invited) GOI Substrates: Fabrication and Characterization. ECS Transactions, 2013, 50, 709-725.	0.3	1
150	Nanoscale-resolved near-infrared photoabsorption spectroscopy and imaging of individual gallium antimonide quantum dots. Journal of Vacuum Science and Technology B:Nanotechnology and Microelectronics, 2014, 32, .	0.6	1
151	Improvement effect of electrical properties in postâ€annealed waferâ€bonded Ge(001)â€ <scp>OI</scp> substrate. Physica Status Solidi (A) Applications and Materials Science, 2014, 211, 601-605.	0.8	1
152	Dislocation behavior of surface-oxygen-concentration controlled Si wafers. Thin Solid Films, 2014, 557, 106-109.	0.8	1
153	Formation of epitaxial nanodots on Si substrates with controlled interfaces and their application. Japanese Journal of Applied Physics, 2015, 54, 07JD01.	0.8	1
154	Study on the influence of different trench-patterned templates on the crystalline microstructure of AlN epitaxial films by X-ray microdiffraction. Japanese Journal of Applied Physics, 2017, 56, 025502.	0.8	1
155	Thermoelectric performances in transparent ZnO films including nanowires as phonon scatterers. Journal of Physics: Conference Series, 2018, 1052, 012126.	0.3	1
156	Formation and Magnetic Properties of Ultrahigh Density Fe3Si Nanodots Epitaxially Grown on Si(111) Substrates Covered with Ultrathin SiO2Films. Japanese Journal of Applied Physics, 2011, 50, 015501.	0.8	1
157	Opto-Electronic Properties of Ge and Si Related Nanostructures on Ultrathin Si Oxide Covered Si Surfaces. Materials Research Society Symposia Proceedings, 2008, 1145, 1.	0.1	0
158	Local Optical Characterization Related to Si Cluster Concentration in GaAs Using Scanning Tunneling Microscope Cathodoluminescence Spectroscopy. Japanese Journal of Applied Physics, 2008, 47, 6109.	0.8	0
159	Self-organization and Self-repair of a Two-dimensional Nanoarray of Ge Quantum Dots Epitaxially Grown on Si Substrates using Ultrathin SiO2 Films. Hyomen Kagaku, 2010, 31, 626-631.	0.0	0
160	Photoabsorption properties of β-FeSi2 nanoislands grown on Si(111) and Si(001): Dependence on substrate orientation studied by nano-spectroscopic measurements. Thin Solid Films, 2011, 519, 8477-8479.	0.8	0
161	Effect of Low-Energy Ga Ion Implantation on Selective Growth of Gallium Nitride Layer on Silicon Nitride Surfaces Using Metal Organic Chemical Vapor Deposition. Japanese Journal of Applied Physics, 2011, 50, 06GC02.	0.8	0
162	Development of Novel System Combining Scanning Tunneling Microscope-Based Cathodoluminescence and Electroluminescence Nanospectroscopies. Japanese Journal of Applied Physics, 2011, 50, 08LB18.	0.8	0

#	Article	IF	CITATIONS
163	Structural change induced in carbon materials by electronic excitations. Proceedings of SPIE, 2011, , .	0.8	0
164	Structural Change during the Formation of Directly Bonded Silicon Substrates. Key Engineering Materials, 2011, 470, 158-163.	0.4	0
165	(Invited) Nanocontact Epitaxy of Thin Films on Si Substrates Using Nanodot Seeds Fabricated by Ultrathin SiO2 Film Technique. ECS Transactions, 2012, 45, 41-45.	0.3	Ο
166	Electron-Beam-Induced Current Study of Electronic Property Change at SrTiO ₃ Bicrystal Interface Induced by Forming Process. Materials Science Forum, 2012, 725, 261-264.	0.3	0
167	High Density Iron Silicide Nanodots Formed by Ultrathin SiO2 Film Technique. Procedia Engineering, 2012, 36, 382-387.	1.2	0
168	Fabrication of Bonded GeOI Substrates with Thin Al2O3/SiO2 Buried Oxide Layers. , 2012, , .		0
169	Characterization of Ge Films on Si(001) Substrates Grown by Nanocontact Epitaxy. , 2012, , .		0
170	Improvement Effect of Electrical Properties in Post-Annealed Wafer-Bonded Ge(001)-OI Substrate. , 2012, , .		0
171	Formation mechanism of peculiar structures on vicinal Si(110) surfaces. Applied Surface Science, 2013, 267, 53-57.	3.1	0
172	Structural analysis of vicinal Si(110) surfaces with various off-angles. Applied Surface Science, 2013, 267, 136-140.	3.1	0
173	Microstructure and interdiffusion behaviour of β-FeSi ₂ flat islands grown on Si(111) surfaces. Journal of Applied Crystallography, 2013, 46, 1076-1080.	1.9	0
174	Epitaxial Growth of Iron-Silicide Nanodots on Si Substrates Using Ultrathin SiO2 Film Technique and Their Physical Properties. ECS Transactions, 2013, 50, 65-70.	0.3	0
175	(Invited) Epitaxial Growth of Nanodots on Si Substrates with Controlled Interfaces and Their Application to Electronics and Thermoelectronics. ECS Transactions, 2014, 64, 91-94.	0.3	0
176	Improvement of current drive of Ge-nMISFETs by epitaxially grown n ⁺ -Ge:P source and drain. , 2014, , .		0
177	Local Strain Distribution in AlN Thick Films Analyzed by X-Ray Microdiffraction. Materials Science Forum, 0, 783-786, 2016-2021.	0.3	0
178	(Invited) Nanostructure Design for Control of Phonon and Electron Transports. ECS Transactions, 2017, 80, 93-100.	0.3	0
179	Keynote Speech: Nanostructure thermoelectrics. , 2019, , .		0
180	Dominant carrier of pseudo-gap antiferromagnet Cr3Al thin film. Physica B: Condensed Matter, 2021, 620, 413281.	1.3	0

#	Article	IF	CITATIONS
181	Development of Novel System Combining Scanning Tunneling Microscope-Based Cathodoluminescence and Electroluminescence Nanospectroscopies. Japanese Journal of Applied Physics, 2011, 50, 08LB18.	0.8	Ο
182	Vacuum-Ultraviolet Light Sources and Their Applications for Processings. Laser-induced Etching of Chlorinated Silicon Surfaces Hyomen Kagaku, 1999, 20, 393-400.	0.0	0
183	Enhancement of Phonon Scattering in Epitaxial Hierarchical Nanodot Structures for Thermoelectric Application. Vacuum and Surface Science, 2018, 61, 296-301.	0.0	Ο
184	Giant Enhancement of Seebeck Coefficient by Deformation of Silicene Buckled Structure in Calciumâ€Intercalated Layered Silicene Film (Adv. Mater. Interfaces 1/2022). Advanced Materials Interfaces, 2022, 9, .	1.9	0